J|A|C|S
ARTICLES
Published on Web 03/29/2007

New Insights into the Mechanism of Triplet Radical-Pair Combinations. The Persistent Radical Effect Masks the Distinction between In-Cage and Out-of-Cage Processes

Carlos A. Chesta,*[,†,‡] Jyotirmayee Mohanty,[§,||] Werner M. Nau,*[,§] Urbashi Bhattacharjee,[†] and Richard G. Weiss*[,†]

Contribution from the Department of Chemistry, Georgetown University, Washington, DC 20057-1227, Departamento de Química, Universidad Nacional de Río Cuarto, 5800-Río Cuarto, Argentina, School of Engineering and Science, Jacobs University Bremen, Campus Ring 1, D-28759 Bremen, Germany, and Bhabha Atomic Research Centre, Mumbai-400 085, India

Received October 23, 2006; E-mail: weissr@georgetown.edu

Abstract: Steady-state and laser-pulsed irradiations of dibenzyl ketone ($ACOB_0$) and derivatives with a *p*-methyl or a *p*-hexadecyl chain ($ACOB_1$ and $ACOB_{16}$, respectively) have been conducted in polyethylene films with 0, 46, and 68% crystallinities. Calculation of the fractions of in-cage combinations of the triplet benzylic radical-pair intermediates based on photoproduct yields, F_c, from $ACOB_{16}$ are shown to be incorrect as a result of the kinetic consequences of drastically different diffusion coefficients for the benzyl and *p*-hexadecylbenzyl radicals. Careful analyses of the transient absorption traces, based upon a new model developed here, allow the correct cage effects to be determined even from $ACOB_0$. The model also permits the rate constants for radical-pair combinations and escape from their cage of origin to be calculated using either an iterative fitting procedure or a very simple one which requires only k_{-CO} and the intensities of the transient absorption immediately after the flash and after the in-cage portion of reaction by the benzylic radicals is completed. Values of the rate constant for decarbonylation of the initially formed arylacetyl radicals, k_{-CO}, have been measured from the rise portions of the laser-flash transient absorption traces. They confirm the assertion from results in liquid alkane media that decarbonylation rates are independent of microviscosity. The data separate components of a reaction from an (in-cage) "cage effect" and an (out-of-cage) "persistent radical effect" that are responsible for formation of AB-type (i.e., decarbonylated) products. The effects here are a consequence of vastly different rates of diffusion for coreacting A· and B· benzylic radicals rather than segregation of the radicals in different parts of a hetereogeneous environment (which leads to an excess of AA and BB products). Heretofore, observation of exclusive formation of AB products has been attributed to in-cage combinations of geminate radical pairs. We show that not to be the case here and provide methodologies which may be used for testing the importance of the "persistent radical effect" component of reaction.

Introduction

Analyses of the chemical fates and dynamic courses of geminate *singlet* radical pairs, generated during photo-Fries reactions of aromatic esters[1] and photo-Claisen reactions of aromatic ethers,[2] have allowed intimate details of in-cage (i.e., cages of origin) and out-of-cage motions to be probed in a variety of media.[3−5] In part, those insights have been possible because in-cage combinations of *singlet* radical pairs are not impeded by spin and enthalpic considerations—every encounter conceptually can lead to products and in-cage combinations can be exceedingly fast.[6] The same is not true of *triplet* radical pairs whose combination requires concomitant intersystem crossing

[†] Georgetown University.
[‡] Universidad Nacional de Río Cuarto.
[§] Jacobs University Bremen.
[||] Bhabha Atomic Research Centre.

(1) (a) Miranda, M. A.; Galindo, F. In *Molecular and Supramolecular Photochemistry*; Ramamurthy, V., Schanze, K. S., Eds.; Marcel Dekker: New York, 2003; Vol. 9, Chapter 2. (b) Miranda, M. A.; Galindo, F. In *CRC Handbook of Organic Photochemistry and Photobiology*, 2nd ed.; Horspool, W. M., Lenci, F., Eds.; CRC Press: Boca Raton, FL, 2003; Chapter 42.
(2) Galindo, F. *J. Photochem. Photobiol., C: Photochem. Revs.* **2005**, *6*, 123−138.
(3) (a) Xu, J.; Weiss, R. G. *Photochem. Photobiol. Sci*. **2005**, *4*, 348−358. (b) Gu, W.; Weiss, R. G. *Tetrahedron* **2000**, *56*, 6913−6925. (c) Xu, J.; Weiss, R. G. *Org. Lett.* **2003**, *5*, 3077−3080. (d) Gu, W.; Warrier, M.; Schoon, B.; Ramamurthy, V.; Weiss, R. G. *Langmuir* **2000**, *16*, 6977−6981.
(4) (a) Warrier, M.; Kaanumalle, L. S.; Ramamurthy, V. *Can. J. Chem.* **2003**, *81*, 620−631. (b) Arumugam, S.; Vutukuri, D. R.; Thayumanavan, S.; Ramamurthy, V. *J. Am. Chem. Soc.* **2005**, *127*, 13200−13206. (c) Kaanumalle, L. S.; Nithyanandhan, J.; Pattabiraman, M.; Jayaraman, N.; Ramamurthy, V. *J. Am. Chem. Soc.* **2004**, *126*, 8999−9006.
(5) (a) Giancaterina, S.; Rossi, A.; Rivaton, A.; Gardette, J. L. *Polym. Degrad. Stab.* **2000**, *68*, 133−144. (b) Sanchez, A. M.; Veglia, A. V.; de Rossi, R. H. *Can. J. Chem.* **1997**, *75*, 1151−1155. (c) Lu, F. F.; Wu, L. Z.; Zhang, L. P.; Tung, C. H.; Zheng, L. Q. *Chin. J. Org. Chem*. **2006**, *26*, 599−609. (d) Gu, W.; Bi, S.; Weiss, R. G. *Photochem. Photobiol. Sci.* **2002**, *1*, 52−59. (e) Tung, C.-H.; Wu, L.-Z.; Zhang, L.-P.; Li, H.-R.; Yi, X.-Y.; Song, K.; Xu, M.; Yuan, Z.-Y.; Guan, J.-Q.; Wang, H.-W.; Ying, Y.-M.; Xu, X.-H. *Pure Appl. Chem*. **2000**, *72*, 2289−2298. (f) Tung, C.-H.; Xu, X.-H. *Tetrahedron Lett.* **1999**, *40*, 127−130.
(6) Nakagaki, R.; Hiramatsu, M.; Watanabe, T.; Tanimoto, Y.; Nagakura, S. *J. Phys. Chem.* **1985**, *89* 3222−3226.

10.1021/ja067461q CCC: $37.00

Scheme 1

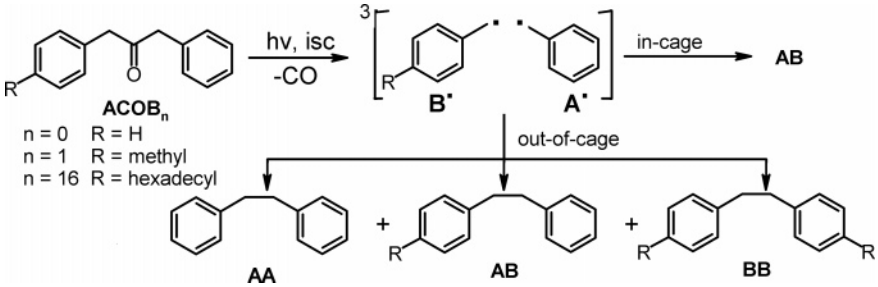

(ISC). Thus, obtaining detailed kinetic information about the in-cage combination of triplet radical pairs involves additional mechanistic considerations and, usually, processes that occur on longer time scales. The generally slower rate of combinations of triplet radical pairs offers additional opportunities and several new experimental challenges.

Dibenzyl ketone ($ACOB_0$) and its derivatives, including those which are asymmetrically substituted with groups on one of the phenyl rings ($ACOB_n$), have been frequently employed as precursors of triplet radical pairs. They have been studied extensively since the discovery by Engel[7] and Robbins and Eastman[8] in 1970 that irradiation of $ACOB_0$ and its derivatives results in a classic Norrish type I process in which the first homolytic step from the triplet state leads to an arylacetyl/benzylic radical pair. Especially in high viscosity organic solvents at room temperature, loss of carbon monoxide from the arylacetyl part is sufficiently rapid to compete with cage-escape by one of the radicals. Thus, a large fraction of the ensuing pairs of benzylic radicals, A•/B•,[9] can be formed in the reaction cavity of their origin while retaining the triplet spin multiplicity of the ketone excited state. The A•/B• pairs either combine within their cage of origin, yielding AB exclusively, or escape and react after reencounters (if no trapping species is present in the medium), yielding principally AA, AB, and BB (Scheme 1).

On the basis of many studies in diverse media and under different stimuli, the nature and kinetics of the motions of A• and B• are thought to be well understood.[10] In fact, the product distributions from combinations of A• and B• have been used by many others[11] and us[12] to assess the abilities of various media to influence translational and rotational motions as well as electron spin interconversions in the presence of external magnetic fields or as a result of isotopic enrichment.[13]

Here, we examine the photochemical reactions of the parent molecule, $ACOB_0$, and two $ACOB_n$ in which a methyl or hexadecyl chain has been appended to the para position of one of the aromatic rings, $ACOB_1$ or $ACOB_{16}$, respectively, within media consisting of *n*-hexane and three types of polyethylenes of different crystallinities. The results from these experiments have allowed us to introduce and to test a model which assesses *quantitatively* the importance of the "persistent radical effect"[14] for small radicals (case 3 of Scheme 2). Analyses of our data according to the model indicate that *the commonly used cage-recombination factor, F_c* (eq 1), *that relates product yields to the fraction of in-cage and out-of-cage combinations by the A•/B• radical pairs, becomes invalid when the rates of diffusion of the radicals are very different.* Thus, the persistent radical effect becomes a dominant process during the photolyses of $ACOB_{16}$.

Scheme 2. Limiting Cases for Combinations of A•/B• Radical Pairs Showing Expected Product Distributions in the Absence of Scavengers

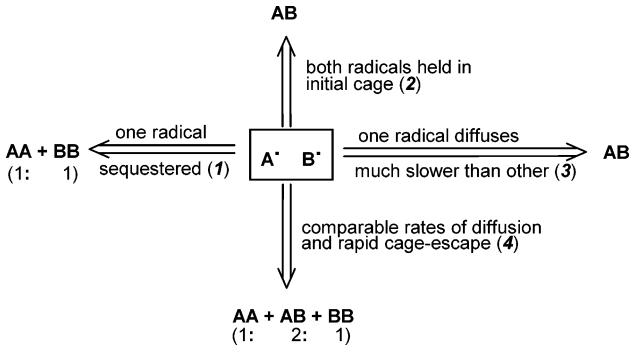

$$F_c = \frac{[AB] - [AA] - [BB]}{[AB] + [AA] + [BB]} \quad (1)$$

The possible scenarios for combinations of A•/B• radical pairs initially in a cage are summarized in Scheme 2. Each has been observed experimentally to some degree. Implicit in the form of eq 1 are the assumptions that 1:2:1 ratios of AA, AB, and

(7) Engel, P. S. *J. Am. Chem. Soc*. **1970**, *92*, 6074−6076.
(8) (a) Robbins, W. K.; Eastman, R. H. *J. Am. Chem. Soc*. **1970**, *92*, 6076−6077. (b) Robbins, W. K.; Eastman, R. H. *J. Am. Chem. Soc*. **1970**, *92*, 6077−6079.
(9) Except as necessary for clarity, the subscript designating the specific nature of the B radicals is omitted.
(10) See for instance: (a) Buchachenko, A. L. *Chem. Rev.* **1995**, *95*, 2507−2528. (b) Tarasov, V.; Ghatlia, N. D.; Buchachenko, A.; Turro, N. J. *J. Phys. Chem*. **1991**, *95*, 10220−10229.
(11) (a) Ruzicka, R.; Barakova, L.; Klan, P. *J. Phys. Chem. B* **2005**, *109*, 9346−9353. (b) Veerman, M.; Resendiz, M. J. E.; Garcia-Garibay, M. A. *Org. Lett.* **2006**, *8*, 2615−2617. (c) Petrova, S. S.; Kruppa, A. I.; Leshina, T. V. *Chem. Phys. Lett.* **2004**, *385*, 40−44. (d) Aspée, A.; Maretti, L.; Scaiano, J. C. *Photochem. Photobiol. Sci*. **2003**, *2*, 1125−1129. (e) Lipson, M.; Noh, T. H.; Doubleday, C. E.; Zaleski, J. M.; Turro, N. J. *J. Phys. Chem*. **1994**, *98*, 8844−8850. (f) Roberts, C. B.; Zhang, J.; Brennecke, J. F.; Chateauneuf, J. E. *J. Phys. Chem*. **1993**, *97*, 5618−5623.
(12) Hrovat, D. A.; Liu, J. H.; Turro, N. J.; Weiss, R. G. *J. Am. Chem. Soc.* **1984**, *106*, 5291−5295.
(13) See for instance: (a) Turro, N. J.; Buchachenko, A. L.; Tarasov, V. F. *Acc. Chem. Res*. **1995**, *28*, 69−80. (b) Step, E. N.; Tarasov, V. F.; Buchachenko, A. L.; Turro, N. J. *J. Phys. Chem*. **1993**, *97*, 363−373. (c) Tarasov, V. F.; Ghatlia, N. D.; Buchachenko, A. L.; Turro, N. J. *J. Am. Chem. Soc.* **1992**, *114*, 9517−9526. (d) Turro, N. J.; Zhang, Z. *Tetrahedron Lett.* **1989**, *30*, 3761−3764. (e) Turro, N. J.; Cheng, C. C.; Wan, P.; Chung, C. J.; Mahler, W. *J. Phys. Chem*. **1985**, *89*, 1567−1568. (f) Gould, I. R.; Turro, N. J.; Zimmt, M. B. In *Advances in Physical Organic Chemistry*; Bethell, D., Ed.; Academic Press: London, 1984; Vol. 20, pp 1−53. (g) Baretz, B. H.; Turro, N. J. *J. Am. Chem. Soc*. **1983**, *105*, 1309−1316. (h) Turro, N. J.; Chung, C.-J.; Lawler, R. G.; Smith, W. J., III. *Tetrahedron Lett.* **1982**, *23*, 3223−3226. (i) Turro, N. J.; Chow, M.-F.; Chung, C.-J.; Kraeutler, B. *J. Am. Chem. Soc.* **1981**, *103*, 3886−3891. (j) Turro, N. J.; Mattay, J. *Tetrahedron Lett.* **1980**, *21*, 1799−1802. (k) Kraeutler, B.; Turro, N. J. *Chem. Phys. Lett*. **1980**, *70*, 270−275. (l) Hwang, K. C.; Roth, H. D.; Turro, N. J.; Welsh, K. M. *J. Phys. Org. Chem*. **1992**, *5*, 209−217.
(14) (a) Bachmann, W. E.; Wiselogle, F. Y. *J. Org. Chem*. **1936**, *1*, 354−382. (b) Perkins, M. J. *J. Chem. Soc.* **1964**, 5932−5935. (c) Fischer, H. *Chem. Rev.* **2001**, *101*, 3581−3610. (d) Studer, A. *Chem.—Eur. J.* **2001**, *7*, 1159−1164.

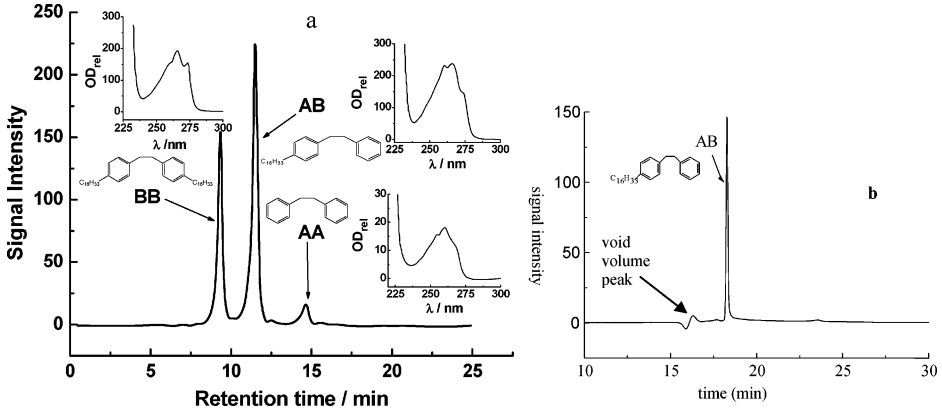

Figure 1. HPLC chromatograms (λ_{det} = 270 nm) of the photoproduct distribution of $ACOB_{16}$ in (a) *n*-hexane and (b) PE46. The UV absorption spectra of the products as obtained in situ from the diode array detector of the HPLC are shown as well. The retention time of $ACOB_{16}$ under the conditions of this chromatogram is ca. 50 min. The AA and BB peaks in spectrum a are not equal in size because their molar extinction coefficients differ at 270 nm.

BB are always obtained from out-of-cage combinations (case 4 of Scheme 2) and exclusive formation of AB signifies complete in-cage reaction (case 2 of Scheme 2). There is an intrinsic ambiguity, therefore, because an excess of AB may result from case 2 or case 3.

The limitations of eq 1 have been recognized qualitatively by Bohne and co-workers who examined the partitioning of radicals from asymmetrically substituted dibenzyl ketones between aqueous and micellar environments,[15] and quantitatively by Turro and co-workers who altered the probabilities of combination of benzylic radicals by placing one inside and another outside zeolite cages during polymerization reactions (case 1 of Scheme 2).[16] Both of these are examples of microphase separation. Although the dependence of the combination of radicals on their relative rates of diffusion in media *without microphase separations* is well documented in polymerization reactions,[14c,17] it is not in photochemical reactions of "small" molecules, such as dibenzyl ketones. Perhaps as a corollary, an easily tractable method for identifying the *true* cage effects in such systems has not been developed.[18]

The model presented here allows the true cage effects to be assessed and the rate constants associated with the various combination steps to be calculated. It removes the mechanistic ambiguity from the limiting cases 2 and 3. Furthermore, it is easily adaptable to a wide variety of reactions and media where the diffusion rates of two radical species are very different (i.e., the "persistent radical effect") or the cage effects cannot be calculated from photoproduct distributions (N.B., $ACOB_0$).

The method relies on analyses of transient absorption kinetics from flash photolyses. We apply it here to calculate the correct fractions of in-cage and out-of-cage combinations by the triplet benzylic radical pairs from $ACOB_0$, $ACOB_1$,[19] and $ACOB_{16}$ which are created in polyethylene (PE) films and to demonstrate the limitations of relying on eq 1.

In addition, a conclusive demonstration of the independence of the rate of decarbonylation of arylacetyl radicals, k_{-CO}, on viscosity in paraffinic media,[20] and an assessment of the dependence of the true F_c on the degree of crystallinity of the polyethylene host and the length of the alkyl chain (R) in the $ACOB_n$ are presented. Although the independence of k_{-CO} on medium viscosity has been inferred from data obtained in liquid *n*-alkanes, it has not been extrapolated to extremely viscous microenvironments, such as those afforded by the polyethylenes.

Results and Discussion

Most experimental details, including the syntheses of 1-(4-hexadecylphenyl)-3-phenyl-2-propanone ($ACOB_{16}$) and its expected photoproducts, are reported in the Supporting Information. Polyethylene films are designated according to their degree of crystallinity: PE0, PE46, and PE68 have 0, 46, and 68% crystallinities, respectively. Their properties have been reported elsewhere.[19,21]

Steady-State Irradiations. Irradiations were conducted at >300 nm, in the long wavelength absorption bands of the $ACOB_n$ (Supporting Figure S1), to produce $^1(n,\pi^*)$ states. Since AA, AB, and BB photoproducts do not absorb at >300 nm, their primary ratios were quantified easily by HPLC (Figure 1a) after correction of the peak areas for detector responses. Photolysis of $ACOB_1$ or $ACOB_{16}$ in *n*-hexane yielded AA, AB, and BB as the only detected photoproducts in a ca. 1:2:1 distribution (i.e., all reaction occurs out-of-cage[22] or with zero cage effect; case 4 of Scheme 2 applies). The values of F_c calculated from the steady-state experiments are collected in

(15) (a) Kleinman, M. H.; Shevchenko, T.; Bohne, C. *Photochem. Photobiol.* **1998**, *68*, 710−718. (b) Kleinman, M. H.; Shevchenko, T.; Bohne, C. *Photochem. Photobiol.* **1998**, *67*, 198−205.
(16) Lei, X.-G.; Jockusch, S.; Ottaviani, M. F.; Turro, N. J. *Photochem. Photobiol. Sci.* **2003**, *2*, 1095−1100.
(17) See for instance: (a) Studer, A. *Chem. Soc. Rev.* **2004**, *33*, 267−273. (b) Fischer, H. In *Advances in Controlled/Living Radical Polymerization;* Matyjaszewski, K., Ed.; ACS Symposium Series 854; American Chemical Society: Washington, DC, 2003, pp 10−23.
(18) Methods that are not generally applicable to monomeric systems or easily amenable to closed solutions are available. See for instance: (a) Fischer, H. *J. Polym. Sci., Part A: Polym. Chem.* **1999**, *37*, 1885−1901. (b) Tang, W.; Fukuda, T.; Matyjaszewski, K. *Macromolecules* **2006**, *39*, 4332−4337. (c) Karatekin, E.; O'Shaughnessy, B.; Turro, N. J. *J. Chem. Phys.* **1998**, *108*, 9577−9585.
(19) Bhattacharjee, U.; Chesta, C. A.; Weiss, R. G. *Photochem. Photobiol. Sci.* **2004**, *3*, 287−295 and references therein.
(20) (a) Tsentalovich, Y. P.; Kurnysheva, O. A.; Gritsan, N. P. *Russ. Chem. Bull. Int. Ed.* **2001**, *50*, 237−240. (b) Tsentalovich, Y. P.; Fischer, H. *J. Chem. Soc., Perkin. Trans.* **1994**, *2*, 729−733. (c) Zhang, X.; Nau, W. M. *J. Phys. Org. Chem.* **2000**, *13*, 634−639. (d) Claridge, R. F. C.; Fischer, H. *J. Phys. Chem.* **1983**, *87*, 1960−1967. (e) Tokumura, K.; Ozaki, T.; Nosaka, H.; Saigusa, Y.; Itoh, M. *J. Am. Chem. Soc.* **1991**, *113*, 4974−4980. (f) Maouf, A.; Lemmetyinen, H.; Koskikallio, J. *Acta Chem. Scand.* **1990**, *44*, 336−338. (g) Turro, N. J.; Gould, I. R.; Baretz, B. H. *J. Phys. Chem.* **1983**, *87*, 531−532. (h) Lunazzi, L.; Ingold, K. U.; Scaiano, J. C. *J. Phys. Chem.* **1983**, *87*, 529−530. (i) Kurnysheva, O. A.; Gritsan, N. P.; Tsentalovich, Y. P. *Phys. Chem. Chem. Phys.* **2001**, *3*, 3677−3682.
(21) Brown, G. O.; Guardala, N. A.; Price, J. L.; Weiss, R. G. *J. Phys. Chem. B* **2002**, *106*, 3375−3382.
(22) (a) Turro, N. J. *Proc. Natl. Acad. Sci. U.S.A.* **1983**, *80*, 609−621. (b) Gould, I. R.; Turro, N. J.; Zimmt, M. B. In *Advances in Physical Organic Chemistry*; Bethell, D., Ed.; Academic Press: London, 1984; Vol. 20, pp 1−53. (c) Turro, N. J. *Chem. Commun.* **2002**, 2279−2292. (d) Turro, N. J. *Acc. Chem. Res.* **2000**, *33*, 637−646.

Table 1. Rate Constants and F_{cAB} Values at 290 K Calculated from Laser-Flash (LF) Photolysis Experiments According to the Model and F_c Values from Steady-State (SS) Photolyses Conducted at 295 K[a]

polyethylene		$ACOB_0$	$ACOB_1$	$ACOB_{16}$
PE0[b]	$k_{-CO}/10^6\ s^{-1}$	4.6 ± 0.5	6.0 ± 0.3	6.2 ± 0.3
		4.7 ± 0.2		
		4.7 ± 0.3[c]		
	$k_{dAB}/10^4\ s^{-1}$	7.4 ± 0.9	7.5 ± 0.9	11.0 ± 0.5
	$k_r/10^4\ s^{-1}$	4.7 ± 0.2	5.0 ± 0.2	5.4 ± 0.2
	F_{cAB}	0.38 ± 0.04	0.40 ± 0.04	0.33 ± 0.01
PE46[d,e]	$k_{-CO}/10^6\ s^{-1}$	4.7 ± 0.7	5.5 ± 0.2	>5[f]
	$k_{dAB}/10^4\ s^{-1}$	8.6 ± 0.9	9.4 ± 0.3	16.0 ± 0.2
	$k_r/10^4\ s^{-1}$	11.0 ± 0.2	11.0 ± 0.1	14.0 ± 0.1
	F_{cAB}	0.55 ± 0.04 (0.55)	0.55 ± 0.05 (0.55)	0.46 ± 0.02
	F_c		0.51 ± 0.03	1.00 ± 0.04
PE68[d,e]	$k_{-CO}/10^6\ s^{-1}$	4.8 ± 0.6	5.6 ± 0.5	>5[f]
	$k_{dAB}/10^4\ s^{-1}$	7.8 ± 0.8	7.4 ± 0.4	13.0 ± 0.4
	$k_r/10^4\ s^{-1}$	9 ± 1	12 ± 1	11.0 ± 0.1
	F_{cAB}	0.53 ± 0.01 (0.54)	0.61 ± 0.07 (0.61)	0.44 ± 0.06 (0.50)
	F_c		0.67 ± 0.04	1.00 ± 0.04
n-hexane[e]	$k_{-CO}/10^6\ s^{-1}$	6.4[20c]		
	F_c		0.01 ± 0.03[19]	-0.01 ± 0.04

[a] Except as indicated, all laser-flash data are averages from 10 laser shots on one spot of an aerated film. In the fitting routines using the model, k_{-CO} was fixed to the values from fits of the rise portions of transient absorption traces. Where reliable values of ΔOD^o_{max} and ΔOD^o_e were available from transient absorption traces, values of F_{cAB} from optical density measurements and eq 9 are included in parentheses. [b] For $ACOB_0$ from one shot-averaged decay trace in each of two different films. [c] Stored for 1 month under an argon atmosphere. [d] For $ACOB_1$ average from four separate shot-averaged decay traces from four different spots on one film. [e] Errors limits are the *t*-test confidence intervals calculated at 95% confidence. [f] No accurate measurement possible because of strong scattering and fast kinetics.

Table 1. In other isotropic liquid media, as well, F_c from $ACOB_1$ is nearly zero.[19]

From a practical standpoint, the presence of some micrometer-range crystalline objects[19,21] in the PE films causes significant scattering of the incident radiation (and some apparent broadening of the absorption bands). For this reason, concentrations of the dibenzyl ketones were approximated by using the molar extinction coefficients in *n*-hexane and setting the baselines with reference to an undoped PE film; for example, see Supporting Figure S2. Irradiations of $ACOB_{16}$ in the PE films at room temperature produced AB exclusively (Figure 1b). $ACOB_1$[19] yielded ratios of AB/(AA + BB) which are much larger than the 1/1 expected statistically: 3.0 in PE46 and 5.1 in PE68.

An excess of AB has been associated traditionally with a mixture of case 2 and case 4 in Scheme 2 and analyzed using eq 1.[22] Accordingly, the exclusive formation of AB from $ACOB_{16}$ in both PE46 and PE68 films would indicate a cage effect of unity, while the photoproduct ratios from $ACOB_1$ would correspond to 67% and 51% cage effects in PE68 in PE46, respectively (Table 1). On the basis of the joint analysis of photoproduct ratios and laser-flash photolysis data, the observed excess of AB in the polymer films is *not* (or not exclusively) a result of the cage effect but rather of the persistent radical effect (case 3 in Scheme 2).[14] Accordingly, the more slowly diffusing B· radicals are trapped preferentially by the more mobile benzyl radicals (A·). Our kinetic model separates, for the first time, the components of the reaction from the in-cage reaction (case 2) and of the persistent radical effect (case 3) that contribute to the excess yields of AB.

These results are in contrast to observations of reduced cage effects (i.e., excess yields of AA and BB photoproducts) or even negative values of F_c according to eq 1 from photolyses of substituted dibenzyl ketones in micelles[15] and zeolites.[23−25] There, microscopic spatial separation of the different species by size or solubility make the probability of collisions between A· and B· very small and favor self-reactions (case 1). Related interpretations based on a separation of reaction space cannot be invoked here because polyethylene films are not microphase-compartmentalized systems (i.e., the entire reaction space outside the crystalline regions is accessible to all solute species). Thus, the walls of the reaction cavities (or cages)[26] afforded by the completely amorphous polymer, PE0, consist of somewhat disorganized polymer chains that are able to relax relatively rapidly[3b] in response to shape changes by the $ACOB_n$. The partially crystalline polymers, PE46 and PE68, place the $ACOB_n$ in a mixture of amorphous and interfacial cages. The latter consist of the lateral edges of lamellar crystallites on one side and amorphous chains on the other; they are thought to be more organized and have higher microviscosities than the completely amorphous cages. However, both types attenuate the rates of diffusion of species such as the $ACOB_n$ and their fragments,[27] and both influence the ability of fragments to move within a cage.[3,26]

Laser-Flash (Pulsed) Irradiations. Laser-flash photolyses of the $ACOB_0$, $ACOB_1$, and $ACOB_{16}$ in the PE films produced transient absorptions (with maxima near 320 nm) which are

(23) Turro, N. J.; Lei, X.-G.; Jockusch, S.; Li, W.; Liu, Z.; Abrams, L.; Ottaviani, M. F. *J. Org. Chem.* **2002**, *67*, 2606−2618.
(24) Turro, N. J.; Lei, X.-G.; Niu, S.; Liu, Z.; Jockush, S.; Ottaviani, M. F. *Org. Lett.* **2000**, *2*, 3991−3994.
(25) In media such as zeolites, rearrangement isomers of dibenzyl ketones have been observed in addition to the products in Scheme 1. We found no evidence for formation of isomers of $ACOB_1$ or $ACOB_{16}$ that would result from recombination of the initial acyl/benzylic radical pairs after irradiations in *n*-hexane or the polyethylene films. (a) Kaanumalle, L. S.; Gibb, C. L. D.; Gibb, B. C.; Ramamurthy, V. *J. Am. Chem. Soc.* **2004**, *126*, 14366−13467. (b) Kaanumalle, L. S.; Nithyanandhan, J.; Pattabiraman, M.; Jayaraman, N.; Ramamurthy, V. *J. Am. Chem. Soc.* **2004**, *126*, 8999−9006. (c) Frederick, B.; Johnston, L. J.; de Mayo, P.; Wong, S. K. *Can. J. Chem.* **1984**, *62*, 403−410. (d) Turro, N. J.; Zhang, Z. *Tetrahedron Lett.* **1987**, *28*, 5637−5640.
(26) (a) Weiss, R. G.; Ramamurthy, V.; Hammond, G. S. *Acc. Chem. Res.* **1993**, *26*, 530−536. (b) Ramamurthy, V.; Weiss, R. G.; Hammond, G. S. In *Advances in Photochemistry*; Volman, D. H., Hammond, G. S., Neckers, D. C., Eds.; Wiley-Interscience: New York, 1993; Vol. 18, pp 67−234.
(27) (a) He, Z.; Hammond, G. S.; Weiss, R. G. *Macromolecules* **1992**, *25*, 1568−1575. (b) Jenkins, R. M.; Hammond, G. S.; Weiss, R. G. *J. Phys. Chem.* **1992**, *96*, 496−502. (c) Lu, L.; Weiss, R. G. *Macromolecules* **1994**, *27*, 219−225. (d) Taraszka, J. A.; Weiss, R. G. *Macromolecules* **1997**, *30*, 2467−2473.

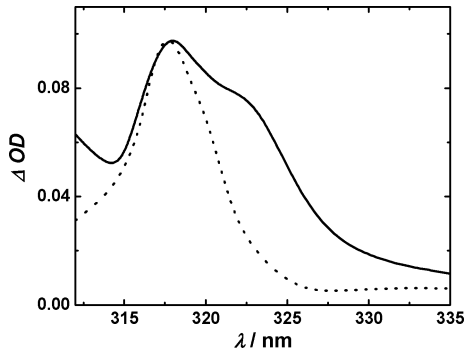

Figure 2. Interpolated normalized transient absorption spectra for benzylic radicals from $ACOB_0$ (···) and $ACOB_{16}$ (—) in 1.4 mm thickness PE0 films. Spectra were obtained in a step-scan mode with 1 nm intervals and after 240 ns ($ACOB_0$) or 400 ns ($ACOB_{16}$) time delays.

characteristic of benzyl and *p*-alkylbenzyl radicals (Figure 2).[20] The spectra resemble closely the previously reported solution spectra (N.B., $\lambda_{max} = 316$ nm for the benzyl radical and $\lambda_{max} = 320$ nm for the *p*-methylbenzyl radical).[20d] A slight bathochromic shift of ca. 1−2 nm and band broadening, which may be due to instrumental settings and/or the polymer matrix, were noted. Spectra from photolyses of both $ACOB_1$ and $ACOB_{16}$ contained a shoulder at 322 nm which is attributed to *p*-alkylbenzyl radicals.

The kinetics of radical decay in the different polymers was monitored at a ca. 5 nm spectral bandwidth which was sufficiently large to allow a satisfactory monitoring light intensity, but sufficiently small to remove most of the scatter from the 308 nm excitation. Scattered light could be almost eliminated for the transparent amorphous PE0 film (Figure 3), but it remained significant for the partially crystalline PE46 and PE68, and was most severe for the latter containing $ACOB_{16}$ (Figure 4a). The interference from scattered light reduced the accuracy of our determinations of k_{-CO}, especially (see later).

The 5 nm spectral bandwidth was too large to permit the decay kinetics of the benzyl and *p*-alkylbenzyl radicals (maxima separated by ~4 nm; Figure 2) to be monitored individually when both were present. Therefore, the monitoring wavelength was set at 320 nm, where the concomitant decay of both species can be followed. This is near the wavelength where their molar extinction coefficients are the same (compare $\epsilon^{316} = 8800 \pm 600$ M^{-1} cm^{-1} for the benzyl radical and $\epsilon^{320} = 7400 \pm 200$ M^{-1} cm^{-1} for the *p*-methylbenzyl radical).[20d]

The transient absorption traces (e.g., Figures 3 and 4) show features in three different time domains: an initial ("instantaneous") rise, a time-resolved rise, and a decay. The initial rise is attributed to the fast homolysis of dibenzyl ketone triplets (i.e., Norrish type I cleavage), yielding a benzylic and arylacetyl radical pair. The time-resolved rise is from formation of additional benzylic radicals as decarbonylation of the arylacetyl radical occurs. The decay is due to the combination of benzylic radicals (as well as trapping of benzylic radicals by molecular oxygen or trap sites within the polymer matrices at much longer times; vide infra).

On the basis of a mechanism in which irradiation of dibenzyl ketones results in cleavage of *one* benzylic-carbonyl bond and the loss of CO proceeds subsequently in a dark reaction (Scheme 3),[20] the ratio of the change of optical densities (ΔODs) for the initial "instantaneous" rise and the protracted rise in the early time portions should be 1:1. In solution phases, the ratio of the initial rise to the time-resolved rise has been reported in some cases to approach 2:1.[20c,g,h] This deviation has been attributed to some photo-induced decarbonylation of arylacetyl radicals during the laser flash.[20c,g,h] In our PE films, the ratio was significantly larger than that in solution (ca. 4:1 in Figure 3a). However, this ratio (as well as the transient kinetics) appeared to be independent of the laser-pulse energies in the range of 40 to 120 mJ; two-photon processes (i.e., secondary photolysis of the initially formed arylacetyl radicals within the laser pulse) do not seem to be the major contributor to the pronounced immediate rise. Alternatively, it has been suggested, although not yet substantiated fully, that the weak tail of the absorption spectrum of arylacetyl radicals may contribute to the immediate rise.[20c,g,h]

Very similar transient traces and decay kinetics were observed when different spots on one polymer film were photolyzed or when the experiments were repeated on the same spot with a second series of laser pulses. The latter comportment was expected because only a very small fraction of the ketone is converted by each laser pulse. Although it was not possible to follow the conversion of starting ketone by UV absorbance changes after one or two pulses, significant decomposition was achieved at high laser energies (>120 mJ) and after >100 laser shots: the samples became more opaque at the irradiated spots and visual inspection of the PE0 samples showed bubble formation, presumably from CO.

Assignment of Rise and Decay Components. Within the time windows covered in Figure 3, fits of the *decay* portions of the traces according to first-order kinetic models (assuming pseudo-unimolecular, in-cage processes) produced more consistent and better fits than when second-order fits (expected for diffusion-dependent, bimolecular, out-of-cage combinations as previously observed in nonviscous solvents[20d]) were employed. The magnitudes of the calculated second-order rate constants ($2k_r$) were unreasonably large ($1-5 \times 10^9$ M^{-1} s^{-1}) given the known rates of self-diffusion of molecules of similar size and shape in polyethylene films.[27,28] Furthermore, the decays from one film that had been equilibrated in air and in argon atmospheres for 1 month prior to pulsed photolyses were indistinguishable over the time scale <20 μs (Figure 5). This observation requires that the kinetics in the viscous polymer matrices is not dictated by bimolecular diffusive processes (such as the radical scavenging by molecular oxygen) on this "short" time scale, but presumably by pseudo-unimolecular in-cage combinations of benzylic radicals. Accordingly, we interpret the protracted rise at <1 μs to decarbonylation of an arylacetyl radical (k_{-CO}) and the decay at <20 μs to in-cage radical-pair combinations (k_r). The values of k_{-CO} will be discussed after an assessment of the decay portions of the traces.

Analyses of Decays of Benzyl Radical Absorbances. The values associated with the decay portions of the transient traces were not directly assigned to the rate constants for in-cage radical pair combinations because it is necessary to include the concurrent cage escape processes. Also, the cage effects as defined by eq 1 and the resulting mechanistic implications provide an inadequate description of the time-resolved experimental data. The contrast is most apparent when the fate of the benzylic radicals is followed on long time scales after a laser

(28) Zimerman, O. E.; Cui, C.; Wang, X.-C.; Atvars, T. D. Z.; Weiss, R. G. *Polymer* **1998**, *39*, 1177−1185.

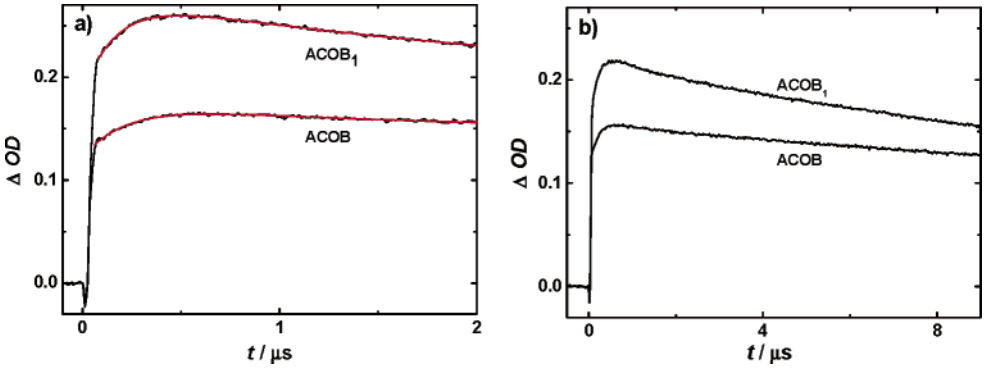

Figure 3. Transient rise and decay profiles at 320 nm upon pulsed irradiation of $ACOB_0$ or $ACOB_1$ in PE0 films over (a) 2 and (b) 8 μs time scales. The fittings of the traces in panel a using a biexponential growth and decay function are shown in red. They were performed to extract the decarbonylation rate constants.

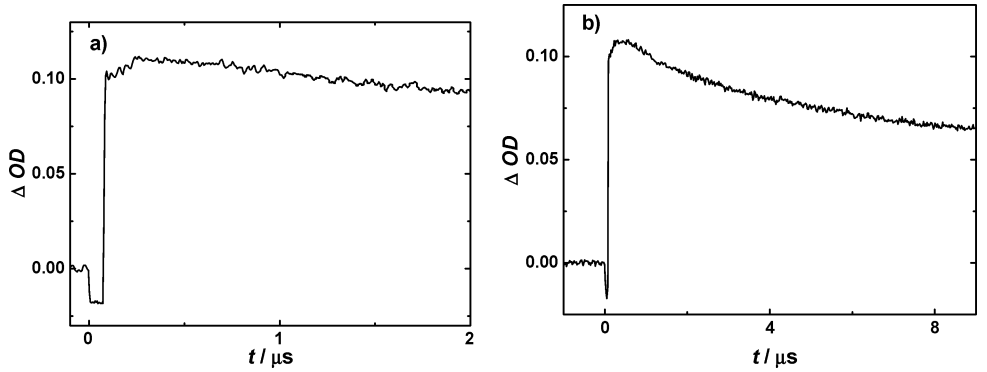

Figure 4. Transient rise and decay profiles at 320 nm upon pulsed irradiation of $ACOB_{16}$ in PE68 at ca. 2 (a) and 8 μs (b) time scales. The ΔOD values after 2 μs do not match in the two traces because they were recorded on different samples.

flash. Thus, if the unity F_c values for $ACOB_{16}$ in the PE films means that all radicals combine in-cage, the transient absorbance should reach a plateau value near zero after no more than a few μs; it does not. Instead, significant transient absorbance extended into the ms time range for all $ACOB_n$ (Figure 5), providing evidence that a significant fraction of radicals had escaped from their original cages. Similar inconsistencies between cage effects calculated by eq 1 and from pulsed transient data were found for $ACOB_1$. On the ms time scale, the observed dynamic quenching by oxygen (Figure 5), which diffuses much more rapidly than the benzylic radicals (vide infra), does not require significant translational diffusion by the benzylic radicals. However, the presence of some AA and BB from $ACOB_1$ does.

The important conclusion at this point is that the large cage effects calculated from the photoproducts according to eq 1 are sometimes inconsistent with much smaller cage effects revealed by transient decay data. An additional factor must be invoked to explain the preferential formation of AB photoproducts from $ACOB_1$ and $ACOB_{16}$ in the PE films. As mentioned above, that factor appears to be the persistent radical effect, which is based on very different diffusion rates for A· and B· (case 3 of Scheme 2).[14]

Decarbonylation Rate Constants. To obtain the values of k_{-CO} in Table 1, the rise and early decay were fitted together using two exponential terms (Figure 3a). The reported values, from at least three independent measurements on three different polymer films, have been corrected for the effects of scattered light where required. As mentioned above, the k_{-CO} values for $ACOB_1$ and $ACOB_{16}$ are weighted averages for phenylacetyl and *p*-alkylphenylacetyl radicals.

The values of k_{-CO} for $ACOB_0$ are known to depend somewhat on solvent polarity.[20a,b] The value for k_{-CO} in PE0, $(4.6 \pm 0.5) \times 10^6$ s^{-1}, is between those reported in *n*-hexane (6.4×10^6 s^{-1}) and in acetonitrile (2.0×10^6 s^{-1}).[20c] More importantly, the similarity of the values in all of the PE films and low viscosity alkane and isoalkane solvents confirms the lack of dependence of k_{-CO} on viscosity that was inferred from studies in *n*-alkanes;[20b,g,h] decarbonylation rates of acyl radicals depend primarily on temperature and the polarity of their immediate environments.[20b,c]

Nevertheless, as expected from results with di-*p*-substituted dibenzyl ketones,[20c−e] the average k_{-CO} values for $ACOB_1$ and $ACOB_{16}$ (i.e., where decarbonylation of a mixture of phenylacetyl and *p*-alkylphenylacetyl radicals is being measured) were ca. 30% higher than that for $ACOB_0$ in PE0. In accordance with the Hammond postulate,[29] alkylation enhances decarbonylation rates because the products, *p*-alkylbenzyl radicals, are more stable than the benzyl radical.[30] Additionally, the degree of crystallinity of the PE matrices had no effect on the k_{-CO} values from $ACOB_0$ and $ACOB_1$; the errors introduced by scattering did not permit the same correlation to be established for $ACOB_{16}$.

Differential Diffusion of Benzylic Radicals. Different rates of radical diffusion should influence the distributions of photoproducts by changing the fraction of in-cage combinations and the distribution of products from out-of-cage combinations. In principle, the transient decays on the millisecond time scale (Figure 4) could have yielded direct information on the mutual diffusion rates and the bimolecular combination rate constants

(29) Hammond, G. S. *J. Am. Chem. Soc.* **1955**, *77*, 334−338.
(30) Vollenweider, J.-K.; Paul, H. *Int. J. Chem. Kinet.* **1986**, *18*, 791−800.

Scheme 3. General Kinetic Scheme Showing all Steps Included in the Fitting Model and Separated in Different Time Regimes[a]

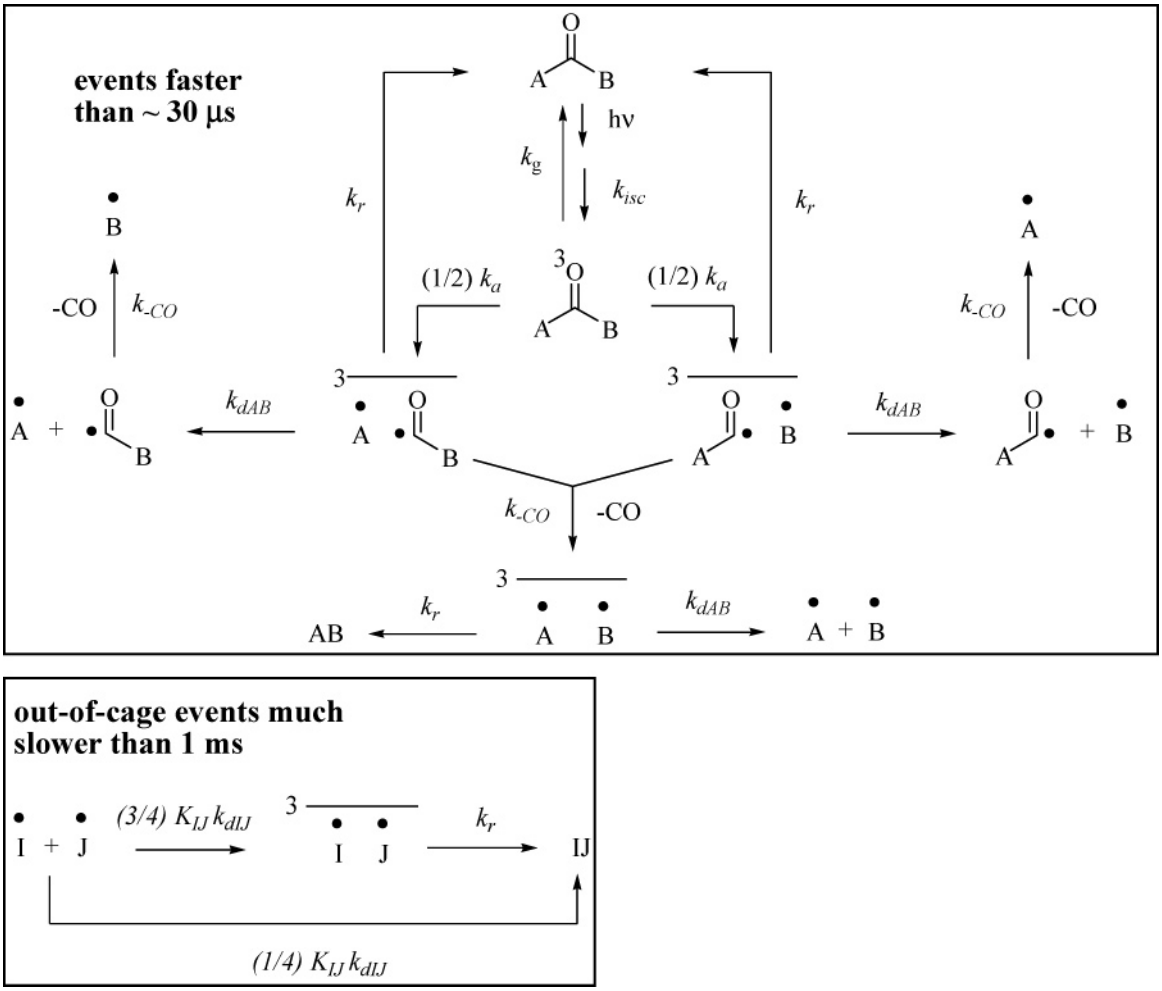

[a] For the steps involving out-of-cage events, I and J represent either fragments A or B. As demonstrated in Supporting Information, no assumptions about the absolute values of the dissociation equilibrium constants, K_{IJ}, are necessary for the interpretation of the experimental data in the <30 μs time regime.

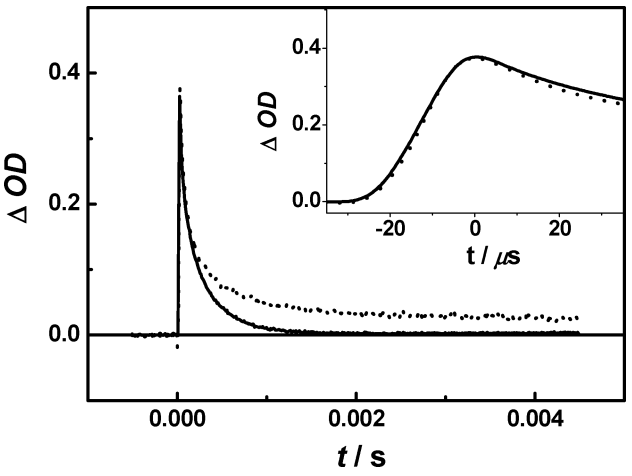

Figure 5. Normalized relative ΔOD transient traces for $ACOB_0$ in a PE0 film that was equilibrated with air (—) and (partially) deoxygenated by leaving it under an Ar atmosphere for 1 month (···). The early time portion of the trace is expanded in the inset.

of the different benzylic radicals. However, since the kinetics of reactive carbon-centered radicals on the millisecond time scale is inevitably affected (and presumably limited) by radical scavengers (molecular oxygen in even the Ar-saturated film and an unknown concentration of polymer trap sites), no further kinetic analysis was attempted. Instead, the diffusive properties of these radicals were estimated.

The benzyl (mass 91) and *p*-methylbenzyl (mass 105) radicals from $ACOB_1$ have nearly identical sizes and shapes, and their mass ratio, 1:1.2, is also very similar. In contrast, the benzyl and hexadecylbenzyl (mass 315) radicals from $ACOB_{16}$, with mass ratio 1:3.5 and very different sizes and shapes, should diffuse at very different rates. For instance, at 25 °C in cyclohexane, the propyl radical (mass 43) has a rate constant for self-termination of 17.0×10^8 M^{-1} s^{-1} and a diffusion coefficient of 8.0×10^{-6} cm^2 s^{-1}, whereas the 1-octadecyl radical (mass 253) values are 4.1×10^8 M^{-1} s^{-1} and 2.7×10^{-6} cm^2 s^{-1}.[31] These values for the diffusion coefficients are ca. one-third those calculated using the Smoluchowski−Einstein model for translational diffusion and suggest that the radicals are associated with the solvent environments more strongly than are the corresponding alkanes.

In general, solvent plays a very important role in governing reactions and reaction pathways. Solute−solvent attractive interactions (i.e., "solvent friction") slow solute diffusion,[32] and benzyl and other radicals move slower than their parent

(31) Burkhart, R. D.; Boynton, R. F.; Merrill, J. C. *J. Am. Chem. Soc.* **1971**, *93*, 5013−5017.
(32) Yamaguchi, T.; Kimura, Y. *Mol. Phys.* **2000**, *98*, 1553−1563.

molecules in both alkane and hydroxylic solvents.[33] Also, the rates of diffusion of small guest molecules in the very viscous polyethylene films are much slower (ca. 10^{-4}) than in a liquid such as *n*-hexane,[27] and the difference between the rates of diffusion of the benzyl and *p*-hexadecylbenzyl radical may be increased further in polyethylene films; diffusion rates of *p*-methylbenzyl and benzyl radicals, produced in the photolysis of $ACOB_1$ are probably very similar even in PE films.

A Kinetic Model Including the Persistent Radical Effect. The mechanism in Scheme 3, which has been used in the quantitative analyses and fittings of the transient traces in the shorter (μs) time domains, is more elaborate than the steps usually invoked.[20] Even so, Scheme 3 is incomplete. It ignores possible consequences from secondary cage effects (i.e., escape by one radical and its subsequent return to the same cage),[34] although such processes are expected in viscous media such as polyethylene. Also, it is applicable only to systems in which diffusion is Fickian.[35] When application of the Smoluchowski equation is not appropriate (e.g., when the radical centers are attached to polymer chains whose repetition controls the motions), more complicated models must be employed.[36] Note that the rate constant, k_r, represents actually the rate of hyperfine coupling-induced intersystem crossing, followed by fast, spin-allowed bond formation.[19] On the basis of the comparable hyperfine coupling constants in the closely related benzylic radicals, we assume that k_r(A+A) and k_r(B+B) are comparable; k_r(A+COA) may be slightly different, but this rate does not affect F_c. The more important simplifications and assumptions bearing directly on the kinetic expressions are listed as follows: (i) The triplet states of the $ACOB_n$ are the immediate precursors of all lysis steps. (ii) Reactions involving formation of the potential photoproducts, ACOA, BCOB, ACOCOA, ACOCOB, and BCOCOB, are neglected because they were not observed in our experiments. (iii) Probabilities for cleavage of the A−C or B−C bonds (k_α) in $ACOB_n$[3] are the same. (iv) The diffusion coefficients *D* for radicals of each pair, A· and ĊOA and B· and ĊOB, are the same because of their similar sizes and shapes. (v) The rate constant for diffusion involving two of radical A· (steps 18, 19, and 20 in Supporting Information) or two of radical B· (steps 22, 23, and 24 in Supporting Information), k_{dAA} and k_{dBB}, respectively, are proportional to the corresponding diffusion coefficients: $k_{dAA} \propto D_A$ and $k_{dBB} \propto D_B$.[37] (vi) Diffusion of a radical A· (or ĊOA) and a radical B· (or ĊOB) can be expressed by an average rate constant: $k_{dAB} = {}^1/_2(k_{dAA} + k_{dBB})$. (vii) The rate constants for all spin-forbidden, triplet radical-pair combinations, k_r, are the same (steps 6, 9, 13, 17, and 21 in Supporting Information).[20c] We note that some of the in-cage processes may, in principle, be influenced by collisions between A·/B· triplet radical pairs and molecular oxygen.[38] However, the fact that the value of k_r is unchanged in the presence and absence of molecular oxygen when $ACOB_0$ is flash irradiated in PE0 (as indicated by the early decay portion in Figure 5) requires that such collisions have a very small influence on the rate of intersystem crossing by A·/B· triplets. (viii) The rate constants for "in-cage" and "out-of-cage" decarbonylation of ĊOR (R = A or B) radicals, k_{-CO}, are the same (steps 7, 9, 11, and 12 in Supporting Information) because the loss of CO is controlled by the environment, temperature, and nature of R of an acyl radical. The environments are very similar, the temperature is constant, and the differences between the decarbonylation rates of phenylacetyl and (*p*-methylphenyl)acetyl (and, presumably, (*p*-hexadecylphenyl)acetyl) are known to differ by ca. 30%,[20c] an amount that is large relatively but small in absolute terms. (ix) Pairs of free radicals combine at rates proportional to their rates of diffusion. (x) Rates of AB, AA, and BB formation from out-of-cage reactions (triplet steps 15, 19, and 23 and singlet steps 16, 20, and 24 in Supporting Information) are determined by spin statistics of radical-pair encounters. Formation of products from the singlet pairs within a cage (k_{fIJ}, where I and J represent either of the benzylic radicals) is not shown explicitly in the mechanism because it is assumed that the rate constant for photoproduct formation from singlet pairs (k_r^1) is much larger than that for cage radical escape (i.e., $k_r^1 \gg k_{dIJ}K_{IJ}$), so that $k_{fIJ} \cong {}^1/_4 k_{dIJ}K_{IJ}$ even in fluid media.[20d,39] (xi) The laser pulses produce a homogeneous distribution of radicals across the irradiated polymer spot. This condition is important for analyses of bimolecular processes. They are not examined per se here.

From Scheme 3 and these assumptions, a set of eight simultaneous differential equations (eqs 25−33 in Supporting Information) can be written to describe the rate processes. If the intensity of radiation absorbed by $ACOB_n$ is invariant with time and conversion (i.e., steady-state photolysis), the concentrations of all of the transient species, including the radical intermediates, are constant (i.e., the steady-state assumption holds), and d[*AB*]/d*t*, d[*AA*]/d*t*, and d[*BB*]/d*t* are equal to constants. Hence, as long as the time required for the intermediates to achieve the steady-state condition is negligibly short compared to that for the total photolysis, F_c can be written as

$$F_c = \frac{(\mathrm{d[AB]/d}t) - (\mathrm{d[AA]/d}t) - (\mathrm{d[BB]/d}t)}{(\mathrm{d[AB]/d}t) + (\mathrm{d[AA]/d}t) + (\mathrm{d[BB]/d}t)} \qquad (2)$$

From eq 2 and the differential equations mentioned above, it

(33) (a) Okamoto, K.; Hirota, N.; Terazima, M. *J. Phys. Chem. A* **1997**, *101*, 5269−5277. (b) Terazima, M.; Okamoto, K.; Hirota, N. *J. Chem. Phys.* **1995**, *102*, 2506−2515.

(34) (a) Rice, S. A. In *Diffusion-Limited Reactions. Comprehensive Chemical Kinetics*; Bamford, C. H., Tipper, C. F. H., Compton, R. G., Eds.; Elsevier: Amsterdam, The Netherlands, 1985; Vol. 25, pp 1−400. (b) Burshtein, A. I. In *Unified Theory of Photochemical Charge Separation. Advances in Chemical Physics*; Prigogine, I., Rice, S. A., Eds.; Wiley: New York, 2000; Vol. 114, pp 419−587.

(35) Crank, J. *The Mathematics of Diffusion*, 2nd ed.; Oxford Press: Oxford, 1975.

(36) (a) Neogi, P., Ed. *Diffusion in Polymers*; Marcel Dekker: New York, 1996. (b) Vieth, W. R. *Diffusion in and Through Polymers*; Hanser: Munich, Germany, 1991.

(37) Smoluchowski, M. v. *Z. Phys. Chem*. **1917**, *92*, 129−168.

(38) The concentration of oxygen (from air) in a PE film is $\sim 4 \times 10^{-4}$ M.[38a] In a low-density PE at room temperature, the diffusion coefficients for toluene (a model which overestimates somewhat the diffusion coefficients of benzyl and *p*-methylbenzyl[32,33]) and molecular oxygen are $\sim 2 \times 10^{-8}$ cm^2/s[38b] and $\sim 4.6 \times 10^{-7}$ cm^2/s,[38c] respectively. Assuming a collision radius (ρ') of 5 Å and $k_{dif} = 4\pi\rho' N(D_1 + D_2)/1000$, a value of $\sim 10^8$ L/mol-s is calculated. Then, the rate of collision of molecular oxygen with a benzylic radical is $\sim 4 \times 10^4$ s^{-1}, somewhat slower than (but comparable to) the rate of the in-cage reactions (k_r) (see Table 1). (a) Michaels, A. S.; Bixler, H. J. *J. Polym. Sci.* **1961**, *L*, 393−412. (b) Saleem, M.; Asfour, A.-F. A.; De Kee, D. *J. Appl. Polym. Sci.* **1989**, *37*, 617−625. (c) Michaels, A. S.; Bixler, H. J. *J. Polym. Sci.* **1961**, *L*, 413−439.

(39) The actual processes for combination of free radicals from the singlet channel are more complex than what is shown here. The simplified expression of the rate constants as ${}^1/_4\ k_{dIJ}K_{IJ}$ in eq 16, 20, and 24 of the model in Supporting Information is warranted because singlet → triplet radical-pair intersystem crossing should be much slower than an in-cage combination, and in-cage combinations of alkyl singlet radical-pairs is a barrierless process that can compete favorably with diffusion even in fluid solutions[39a,b] (and, therefore, certainly in our PE films). (a) Strauss, O. P.; Lown, J. W.; Gunning, H. E. in *Comprehensive Chemical Kinetics*; Bamford, C. H., Tippen, C., Eds.; Elsevier: Amsterdam, The Netherlands, 1973; Vol. 5, p 566 and references therein. (b) Ward, H. R. *Acc. Chem. Res.* **1972**, *5*, 18−24.

can be shown that

$$F_c = \frac{F_{cAB} + R_-(1 - F_{cAB})}{F_{cAB} + R_+(1 - F_{cAB})} \quad (3)$$

where F_{cAB} (eq 4) is a cage effect factor and R_- and R_+ (eqs 60 and 61 of Supporting Information) are complex expressions defined in Supporting Information.

$$F_{cAB} = \left(\frac{k_r}{k_r + k_{dAB}}\right)\left(\frac{k_{-CO}}{k_{-CO} + k_{dAB}}\right) \quad (4)$$

There are two practical limiting conditions for F_c:

(1) Radical A· is the same as radical B· (as in the case of irradiations of $ACOB_0$), so that $k_{dAA} = k_{dBB}$, $R_- = 0$, $R_+ = 1$, and $F_c = F_{cAB}$. It is not possible to measure F_c experimentally from the product yields of $ACOB_0$ since AA, AB, and BB have the same molecular structures. However, because of the similar structures and diffusivities of A· and B· from $ACOB_1$, the approximation that $k_{dAA} \cong k_{dBB}$ should be valid and F_{cAB} values from laser-flash experiments (vide infra) should be almost the same as those for F_c from steady-state irradiations (i.e., the relative yields of AA, AB, and BB).

(2) When A· and B· have very different rates of diffusion, so that the value of F_c can be evaluated in the limit, $k_{dBB}/k_{dAA} \rightarrow 0$ (taking arbitrarily $k_{dAA} \gg k_{dBB}$, in keeping with the nature of B· from $ACOB_n$ when n is a large number). To do so requires an estimation of the partial limits of the three terms in each expression for R_- and R_+.

$$\mathrm{Lim}_{k_{dBB}/k_{dAA}\rightarrow 0}(F_c) = \frac{F_{cAB} + R_{lim}(1 - F_{cAB})}{F_{cAB} + R_{lim}(1 - F_{cAB})} = 1 \quad (5)$$

Equation 5 (eq 72 of Supporting Information), the product of that exercise, leads to the prediction that *if $k_{dAA} \gg k_{dBB}$, F_c approaches unity independent of the absolute values of k_{dAA} and F_{cAB}.* Consequently, the value of F_c (calculated from steady-state photoproduct yields and eq 1) is not the true cage effect factor as a direct consequence of the unequal diffusivities of radicals A· and B· and the resultant enhancement of "out-of-cage" formation of AB.

This situation is tantamount to "the persistent radical effect" (case 3 in Scheme 2).[14] Conceptually, the low diffusivity of B· makes the probability of it finding another radical B· very small. As a result, the concentration of B· in the photostationary state will exceed that of radical A·. Also, the diffusion rate constant associated with the formation of AB (k_{dAB}) is not dramatically affected when $k_{dAA} \gg k_{dBB}$: although a radical B_n· (where n is large and (k_{dBB}/k_{dAA}) $\rightarrow 0$) can be considered as "static" during its lifetime in a very high viscosity medium (such as a PE matrix), the high mobility of radicals A· allows them to diffuse to sites occupied by radicals B· to produce AB because $k_{dAB} = k_{dAA}/2$. Hence, although the large accumulation of B· in the photostationary state of a constant intensity irradiation experiment favors the formation of BB, it is offset by the relatively small value of k_{dBB}; although k_{dAA} is large, the formation of AA is offset by the small $[\dot{A}]^2$. As a result, the efficiency of out-of-cage formation of AB is greatly enhanced, independent of the value of the true cage effect factor F_{cAB}.

The reason why F_{cAB} always represents a true cage effect factor while F_c does not, becomes apparent after analyzing the equations as is done in Supporting Information. In essence, F_{cAB} is a function of the rate constants, k_{dAB}, k_r, and k_{-CO} (eq 4), and it calculates the efficiency of escape of the *geminate* radical pairs from their initial cages. If $k_{dAB} \gg k_r$ or $k_{dAB} \gg k_{-CO}$ (or both), $F_{cAB} = 0$; if some "in-cage" radical-pair combination occurs, $F_{cAB} > 0$ (i.e., AB is more than 50% of the total photoproduct population), and 100% of the in-cage combination corresponds to $F_{cAB} = 1$. In contrast, the generalized expression of F_c measures *all* possible routes to form AB, including those resulting from differences between the diffusion coefficients of A· and B·. As noted previously, $F_c = F_{cAB}$ only if $k_{dAA} = k_{dBB}$. It is also clear that if $k_{dAA} \neq k_{dBB}$ and the radicals are not separated in different microspaces within the medium, $F_c > F_{cAB}$.

Analyses of Laser-Flash (Pulsed) Irradiations of Dibenzyl Ketones. It is apparent that the concentrations of the reaction intermediates, as well as the concentrations of the photoproducts, are time dependent in pulsed experiments, and the value of F_c is time dependent also (i.e., $F_c(t)$). Obtaining an analytical expression for $F_c(t)$ is a formidable task, requiring the solution to the eight simultaneous differential equations (eqs 25−33) in Supporting Information. It is possible to discern more easily the qualitative changes in F_c that occur over time from preliminary analyses of the transient absorption traces.

Immediately after a laser pulse, a defined number of radical pairs is created. In the short (ca. 0−20 μs) time interval, $F_c = 1$ because the only radical combination processes that occur are in-cage. Only at later times, when cage-escaped radicals encounter each other, do AA and BB photoproducts begin to appear. Hence, in the first 20 μs after a laser pulse, $F_c \geq F_{cAB}$ even when $k_{dAA} = k_{dBB}$! In the longer time regime, radicals combine to give AA, AB, and BB in a 1:2:1 statistical ratio if $k_{dAA} = k_{dBB}$. Under these conditions, AA and BB accumulate as the reaction proceeds, but since out-of-cage product formation leads to [AB] = [AA] + [BB], the value of F_c will approach that of F_{cAB} as time progresses and the two will be equal at time = ∞ (practically, less than 100 ms after the laser pulse). This case applies exactly to $ACOB_0$ and approximately to $ACOB_1$.

However, if $k_{dAA} \gg k_{dBB}$, as in the case of $ACOB_{16}$, a vastly different scenario unfolds with time. Again, in the very early time regime, (Δt_1), $F_c(\Delta t_1) = 1$. As time progresses (for a short transient period, Δt_2), some of those radicals A· which have not combined with a radical B· will escape more easily from their cages of origin and encounter other A· or B· radicals to yield AA or AB via out-of-cage combinations. Because A· reacts with itself and B· in this time regime, while the self-reaction pathway for B· is severely attenuated because of its limited mobility, the concentration of B· will increase rapidly. As a consequence, the concentration of the slower moving (and, therefore, more slowly combining) B· will increase rapidly. During the next transient period (Δt_3), radicals A· are confronted with a large excess of radicals B·, so that the formation of AB is much more probable than formation of AA and BB (i.e., $F_c(\Delta t_3) = 1$). Only during the final stages (Δt_4), when nearly all radicals of A· have reacted (mainly with B·), are the remaining unreacted radicals B· expected to form BB. Thus, during two transient periods, *apparent* $F_c(\Delta t)$ values are predicted to be very small or even negative as a result of temporal concentration excesses of A· or B·. Ideally, in the

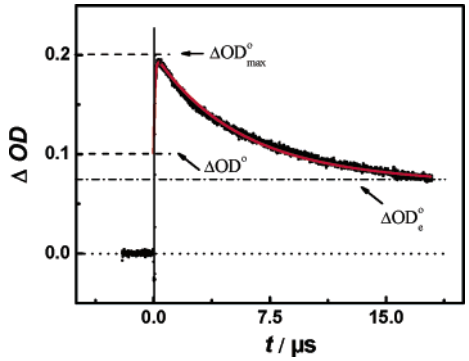

Figure 6. Transient absorption profile monitored at 320 nm for laser-pulsed photolysis of $ACOB_1$ in PE68 at 293 K (black) and the best fit according to our model (red), as well as the estimated values of ΔOD^0, ΔOD^0_{max}, and ΔOD^0_e.

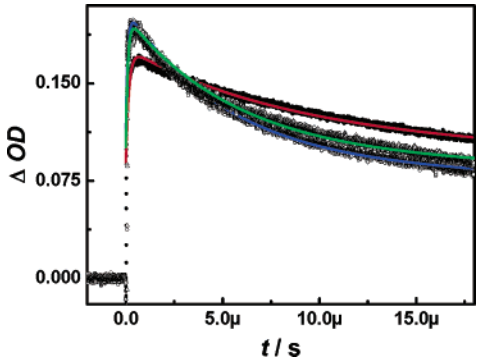

Figure 7. Transient absorption profiles (black) monitored at 320 nm for laser-pulsed photolysis of $ACOB_0$ and best fits according to the fitting model; PE0 (red), PE46 (blue), and PE68 (green) at 293 K.

absence of radical scavengers, the concentration of AA (formed mainly during Δt_2) should equal the concentration of [BB] (formed mainly during Δt_4) when the concentrations are summed over all times after a laser flash.

Although these mechanistic peculiarities cannot be established in experimental detail with our current techniques, F_{cAB}, which always gives the true cage effect factor, is obtainable by applying our model to the transient absorption traces in the 0−20 μs time regime, either by fitting the traces or from the graphically calculated absorptions (see below).

Application of the Model. As noted above, preliminary analyses of our laser-flash data clearly indicate (as expected) that the decays in the transient traces derive from in-cage, first-order combinations of the benzylic radicals at earlier times and from second-order, out-of-cage combinations (as well as pseudo-first-order scavenging processes) at later times. Fortunately, for fitting purposes, the in-cage combinations in the PE films are well separated in time from the other decay processes. α-Cleavage and acyl decarbonylation are virtually complete in <2 μs, and triplet radical-pair combinations and radical escape from geminate reaction cages proceed in the 0−20 μs time period.

By applying our model to the events occurring within the first 20 μs after the ns-duration laser pulses, all terms representing second-order radical combination processes in eqs 25−33 in Supporting Information can be ignored, allowing the simplified equations to be solved. Thus, the transient traces can be fitted empirically[40] according to Scheme 3 to obtain the rate constants needed to calculate F_{cAB}. The values of k_{-CO}, determined from the rise portions of the transient traces, are kept constant while k_r and k_{dAB} are varied. Figure 6 is a typical transient absorption profile and fit. Other examples showing fits to transient absorptions from irradiations of $ACOB_0$ and $ACOB_{16}$ in PE0, PE46, and PE68 are included in Supporting Information.

As is seen in Figure 6, the sharp initial increase in the absorbance (as well as interference from scattered light up to 50 ns after the laser pulses, in particular for the crystalline samples) did not allow the ΔOD at $t = 0$ (ΔOD^o) to be estimated with reasonable precision. However, a value of ΔOD^0 can be calculated from the extrapolated zero-time absorbance maxima in the traces (ΔOD^0_{max}) according to eq 6 (eq 84 of Supporting Information), where $\theta_r = k_r/(k_{-CO} + k_r + k_{dAB})$.

$$\Delta OD^o_{max} = 2(1 - \theta_r)\Delta OD^o \qquad (6)$$

In fluid media, it is reasonable to assume that $k_{dAB} \gg k_r + k_{-CO}$, and therefore the 1:1 ideal relationship should be nearly achieved. In the polyethylene films, we have shown previously[3b] (and our data fits indicate) that $k_{-CO} \gg k_r + k_{dAB}$ and, therefore, the absorption profiles also show a similar behavior. In practice, we estimate ΔOD^0_{max} graphically from the transient absorption traces, and this value is used to calculate an initial estimate of ΔOD^0. The value of ΔOD^0 is adjusted during the process to optimize the fit to a transient absorption profile. Table 1 contains the optimized values of k_r, k_{dAB} and F_{cAB} from these fits.

Approximate values of F_{cAB} can be calculated also from the (graphically) estimated values of ΔOD^0_{max} and ΔOD^0_e (Figure 6). In the long-time regime (at least 20 μs after a laser pulse), the absorbance is due mainly to free radicals A· and B· (eq 7). Thus, eq 8 can be written, and, after appropriate treatment, it becomes eq 9 (eqs 88 and 94 of Supporting Information).

$$\Delta OD \cong \epsilon l\{[\dot{A}] + [\dot{B}]\} \qquad (7)$$

$$\frac{1}{\Delta OD} - \frac{1}{\Delta OD^o_e} \cong \frac{k_{dAB}K_{AB}}{\epsilon l}t \qquad (8)$$

$$F_{cAB} = 1 - \frac{\Delta OD^o_e}{\Delta OD^o_{max}} \qquad (9)$$

The implicit advantage of eq 9 over the fitting routine (vide infra) is that F_{cAB} can be estimated directly from knowledge of only the maximum absorbance extrapolated at time zero (ΔOD^o_{max}) and the absorbance from the total concentrations of benzylic radicals which escape from their initial cages (ΔOD^o_e). In practice, despite the residual absorbance from benzylic radicals undergoing second-order combinations (i.e., benzylic radicals which escape from their geminate cage and react very slowly), ΔOD^o_e should not differ substantially from the absorbance in the plateau and, therefore, can be taken directly from the transient absorbance traces as shown in Figure 6.

(40) Fitting of the experimental transient absorption traces was performed using the generalized reduced gradient (GRG2) nonlinear optimization code. Lasdon, L. S.; Warren, A. D.; Jain, A.; Ratner, M. *ACM Trans. Math. Software 4*; Association for Computing Machinery: New York, 1978; pp. 34−50.

However, as shown in Figure 7, this approach is not always possible. The calculated values of F_{cAB} for $ACOB_0$ in PE46 (blue curve) and PE68 are nearly the same (~0.55 and 0.54, respectively) using both methods. However, there is no obvious way to estimate ΔOD^o_e from the decay for PE0 (red curve). In this case, our simulation of the decay portion of the trace using the parameters obtained from the iterative fitting method suggests that the plateau region is achieved only after 25−30 μs. Thus, the actual period over which the transient traces need be recorded to employ eq 9 must be determined empirically for each sample. Regardless, when reliable values of ΔOD^o_{max} and ΔOD^o_e are available, the values of F_{cAB} calculated by fitting the whole trace and using eq 9 are the same within experimental error. This practical observation is reassuring because it indicates the internal consistency of the model.

General Considerations and Conclusions. The data in Table 1 are reasonable and self-consistent. Note that k_{-CO} is impervious to the degree of crystallinity of the PE matrices and matches the values found in fluid solutions of similar polarity, where such comparisons are possible.

The k_r from one of the $ACOB_n$ did increase between the completely amorphous PE0 and partially crystalline (PE46 and PE68) films, but the differences among the k_r values in one PE film for the 3 $ACOB_n$ are nearly the same. The tentative conclusion from these data is that the in-cage radical combination rates may increase slightly in more confining environments. Small changes in the rates of in-cage combination of *singlet* radical pairs (generated by irradiation of aromatic esters) have also been observed when the crystallinity of the PE media is changed.[3b] In those cases, in-cage combinations must involve rotational as well as translational motions within a cage. A combination of A·/B· radical pairs requires only (but is not limited to) rotational motions.

Crystallinity is only one of several factors that contribute to the nature of the sites of PE in which radical pairs combine.[41] The k_r in Table 1 are 2−3 orders of magnitude lower than the analogous values obtained for the combination of singlet radical pairs in the same media.[3] Since the singlet radical pairs from the aromatic esters are similar in size to the A·/B· from the $ACOB_n$, and the steric requirements for combination of the singlet pairs are more severe than those of the A·/B· triplets, the rate-limiting process for in-cage combination of the triplets must be intersystem crossing.[19]

The lower k_r in PE0 than in PE46 and PE68 is consistent with our prior observations that 'stiffer' walls of reaction cages, such as those in interfacial regions of the partially crystalline PEs, force pairs of radicals to interact more intimately than when the walls are softer (as in amorphous regions of a PE).[3] An additional contributor may be ordering effects of the pairs of benzylic radicals imposed in interfacial regions. If held preferentially on the surface of a crystallite,[42] an A·/B· pair would be able to find an appropriate orientation for combination through in-plane rotational motions only.

The larger value of k_{dAB} for $ACOB_{16}$ than for $ACOB_0$ or $ACOB_1$ in the 3 PE films may be indicative of more than one type of cage even within the amorphous regions. We conjecture that the $ACOB_{16}$, because of strong London dispersive interactions with long, unbranched segments of the polymer chains, are able to reside preferentially in cages which differ somewhat from those preferred by $ACOB_0$ and $ACOB_1$. If that is correct, what appears to be faster random diffusional motion over an average distance by a *p*-hexadecylbenzyl radical may, in fact, be slower directed motion over shorter distances. Some hints that this may be the case come from related observations in photo-Fries reactions of 4-dodecylphenyl phenylacetate in PE films.[43] To address this issue and to determine the chain length at which the limiting conditions for R_- and R_+ no longer hold, future studies will include measurements of rates and cage effects from radical pairs of $ACOB_n$ where $16 > n > 1$. Regardless, it is gratifying that the values of F_c and F_{cAB} are the same in some cases and differ in others as would be predicted conceptually by the model.

From a practical standpoint, the model allows kinetic data for reactions by radicals which diffuse at very different rates within a "single-phase" medium to be analyzed quantitatively. It fills a large gap in our ability to understand and exploit the "persistent radical effect" in a wide range of reactions and media. Although applied here to the photolyses of dibenzyl ketones, the model is applicable to many other reactions, including some involving nonradical intermediates and faster singlet-radical pair combinations.

In conclusion, reliance on product distributions using the customary equation for calculating F_c based on product yields does not always provide the true cage effect. The model developed and applied here does. It is quite tractable whenever diffusion of the intermediate radicals is Fickian. Unfortunately, it is not a substitute for models which treat polymerizations where radicals diffuse in non-Fickian motions.[14,18] Finally, we note that even apparently simple, well-established photochemical systems may have hidden complexities which can lead to erroneous conclusions.

Acknowledgment. This article is dedicated to Professor Chen-Ho Tung of the Technical Institute of Physics and Chemistry and the Institute of Chemistry of the Chinese Academy of Sciences on the occasion of the 70th anniversary of his birth. We thank Dr. Chuping Luo for performing some of the XRD experiments. R.G.W. thanks the U.S. National Science Foundation (NSF) for its support of the research performed at Georgetown. Georgetown University, CONICET, NSF, and the Universidad Nacional of Río Cuarto are thanked by C.A.C. for enabling his sabbatical year at Georgetown. W.M.N. thanks the International University Bremen for support within the graduate program, "Nanomolecular Science." The authors also express their gratitude to the reviewers for several important suggestions and constructive criticisms.

Supporting Information Available: A detailed Experimental section and a complete derivation of the kinetic models for treatment of steady-state and laser-flash derived data. This material is available free of charge via the Internet at http://pubs.acs.org.

JA067461Q

(41) (a) Gu, W.; Hill, A. J.; Wang, X.; Cui, C.; Weiss, R. G. *Macromolecules* **2000**, *33*, 7801−7811. (b) Xu, J.; Weiss, R. G. *J. Org. Chem*. **2005**, *70*, 1243−1252.

(42) (a) Wang, C.; Xu, J.; Weiss, R. G. *J. Phys. Chem. B* **2003**, *107*, 7015−7025. (b) Konwerska-Hrabowska, J. *Appl. Spectrosc*. **1985**, *39*, 434−437. (c) Jang, Y. T.; Phillips, P. J.; Thulstrup, E. W. *Chem. Phys. Lett*. **1982**, *93*, 66−73. (d) Parikh, D.; Phillips, P. J. *J. Chem. Phys.* **1985**, *83*, 1948−1951. (e) Phillips, P. J. *Chem. Rev.* **1990**, *90*, 425−436.

(43) Luo, C.; Passin, P.; Weiss, R. G. *Photochem. Photobiol*. **2006**, *82*, 163−170.